Novel all-cellulose composite displaying aligned cellulose nanofibers reinforced with cellulose nanocrystals

WASHINGTON LUIZ ESTEVES MAGALHÃES, XIAODONG CAO, MAGALY ALEXANDRA RAMIRES, AND LUCIAN A. LUCIA

ABSTRACT: Aligned cellulose nanocrystals/cellulose coelectrospun nanofibers were successfully prepared by using a home-built coelectrospinning and collection system. Cellulose I was dissolved in N-methyl morpholine oxide at 120°C and diluted with dimethyl sulfoxide, which was used in the external concentric capillary needle as the sheath (shell) solution. A cellulose nanocrystal suspension obtained by sulfuric acid hydrolysis of cotton fibers was used as the core liquid in the internal concentric capillary needle after transferring from water to dimethyl sulfoxide. The resultant coelectrospun nanocomposite films were collected onto a rotating wire drum and were characterized by field emission scanning electron microscopy (FE-SEM), Fourier transform infrared spectroscopy, thermogravimetric analysis, and tensile measurements. The FE-SEM image showed that the cellulose nanocrystals did not appear to cluster in the film formed. Although the crystallinity index of nanocomposite fibers was lower than the unreinforced cellulose electrospun fibers, the cellulose type II reinforced with cellulose nanocrystals had a much higher tensile stress (about 140 MPa), almost twofold that of pure cellulose. This latter result indicated that the alignment and adhesion of amorphous cellulose nanofibers played a crucial role on the mechanical properties of electrospun cellulosic fiber mats.

Application: Alignment of fibers plays a crucial role in the overall physical properties of electrospun fiber mats, similar to what is observed in the formation of paper sheets from individual fibers. From a commercial perspective, this has strong implications when considering a material's desired properties.

Cellulose is one of the most abundant biopolymers in the world. It has the attractive characteristics of being both recyclable and renewable. Many researchers in the materials community are interested in its potential use in developing physically strong, robust materials that have low environmental impact. Although the mechanical strength of cellulose nanocrystals has been theoretically predicted to be as strong as or greater than many stainless-steel alloys, there has been no consensus on the value of such mechanical properties. For crystalline cellulose types II, IIII, IIIII, and IV, some authors have predicted modulus of elasticity (MOE) values of 88, 87, 58, and 75 GPa, respectively [1]. Others have calculated the MOE of cellulose types I, II, IIII, and IVI to be 90, 75, 115 and 54 GPa, respectively [2]. Atomic force microscopic measurements on isolated cellulose nanocrystals have found different results for cellulose type I that range between 18 and 50 GP[3]; nevertheless, these values are extremely high.

Until now, it has been impossible to make a macroscopic sample of cellulose crystal that approached the individual unit cell (nanocrystal) mechanical properties; thus, the impressively high calculated and recorded values of the stiffness of crystalline cellulose were not at all useful. Researchers interested in mechanical properties were only able to rely on withdrawing solely the cellulose nanowhiskers from lignocellulosic biomass using relatively facile processes that produced them in water suspensions. To take advantage of the intrinsically high strength of biomass-based cellulose nanocrystals, one approach has been to apply them as reinforcement agents in polymer matrix composites. A new class of cellulosic materials has been developed with the advent of new solvent systems for cellulose. For example, until recently, complete cellulose dissolution using traditional solvents (e.g., N-methyl morpholine oxide [NMMO]) only allowed the mixture amorphous and crystalline type II form of cellulose to be regenerated. It is well known that such cellulose generated from a complete dissolution process exhibits a fraction of the MOE value compared with the allomorphic crystal form. However, several researchers have succeeded in making an all-cellulose composite by partial dissolution of cellulose to achieve MOE values as high as 33 GPa. Notwithstanding, this result can be achieved immediately following alignment of the cellulose chains via wet film stretching and subsequent drying [5, 6].

We have determined that the reinforcement effects of cellulose can be easily attained when the solvent of the matrix polymer is the same as the solvent used to suspend the cellulose nanocrystals. For instance, an all-cellulose composite was obtained by vigorous mixing of a cellulose nanocrystal water suspension into a cellulose sodium hydroxide/urea water solution [7]. Using this process, the all-cellulose composite achieved 157 MPa and 5 GPa for tensile strength and elastic modulus, respectively. In our previous work, we had shown

a methodology to produce all-cellulose composites using coelectrospinning [8], a technique encompassing the use of concentric needles with a cellulose solution in the sheath and a cellulose nanocrystals suspension in the core. With a simple upgrade to the latter technique, we obtained well-aligned cellulose films containing well-dispersed cellulose nanocrystals to achieve high strength.

Our main objective was to describe a new process for obtaining an all-cellulose nanocomposite using coelectrospinning, which involves pulling a submicrometer yarn characterized by a regenerated and aligned cellulose component in the sheath volume space and well-dispersed nanocrystalline cellulose in the core volume space.

EXPERIMENTAL

Materials

N-methyl morpholine oxide and dimethyl sulfoxide (DMSO) (Sigma Aldrich, St. Louis, MO, USA) were used as received to dissolve cellulose from fully bleached eucalyptus pulp (Bahia Sul Celulose S.A., Bahia, Brazil).

Preparation of cellulose nanocrystals

The main steps in the cellulose nanocrystals preparation were (1) acid hydrolysis (64% H_2SO_4, 55°C, 2 h), (2) refining and purification of the solid residue remaining after the hydrolysis by repeated 20–40 min cycles of ultra centrifuging at 7000 rpm followed by resuspension of the solids in distilled water until a turbid supernatant was obtained, and (3) dialysis against distilled water to pH 6–7. A cellulose nanocrystal suspension in DMSO was obtained by solvent exchange from the nanocrystal water suspension by using rotation evaporation.

Preparation of electrospun cellulose nanocrystals-reinforced cellulose nanofibers

Pure cellulose nanofibers, which can be produced using only electrospinning of cellulose-doped solution, were compared against generating neat cellulose composites produced by coelectrospinning. In all of the electrospinning experiments, a 21-gauge needle was used, and the distance from tip to wire rotate drum collector was 10 cm.

For the coelectrospinning experiments, a home-built apparatus was used. The description and operation of the apparatus has been described elsewhere [8]. The volume ratio of the sheath solution to the core suspension is dictated by the relationship between the diameter sizes of the syringes when using the same syringe pump. According to past work [9], the internal needle should extend outside the aluminum hollow cylinder by half the value of the core syringe internal diameter. Thus, in this case, the tap was controlled so that 0.5 mm of the internal needle extended beyond the aluminum hollow-cylinder tip. This procedure assured that the fiber produced by the applied high voltage would extrude around the core suspension. A heat gun blew hot air to heat the needles to approximately 120°C to ensure uniform flow. This temperature was measured using a thermometer before the high voltage was applied.. The sheath and core tip were then connected to a high-voltage power supply (gamma).

A wire drum was constructed that was 8 cm in diameter and 10 cm in length. The wire drum rotated at 300 rpm over water vapor. This collector allowed for the facile regeneration of a more uniform film of cellulose. A cellulose-doped solution of 2 wt% and 3 wt% in NMMO was inside the sheath, and a nanocrystal suspension in DMSO at 1.56 wt% was inside the core.

Characterization

All analyzed samples were obtained as small mats and were coated by a thin 8–10 nm layer of sputtered gold/palladium (Au/Pd). The samples were analyzed using a JEOL JSM-6400F field emission scanning electron microscope (FE-SEM) (JEOL Ltd., Tokyo, Japan) that allowed for high resolution (15–70 Å); images were acquired using a 4pi Universal Spectral Engine (4pi Analysis Inc., Durham, NC, USA).

A Thermo Nicolet NEXUS 670 Fourier transform infrared (FTIR) spectrometer (ThermoFisher Scientific, Waltham, MA, USA) was used to obtain infrared spectra of the mats in transmission mode. The spectra were collected at 4 cm^{-1} interval over the range 4000–650 cm^{-1}. A crystallinity index was defined as $CrI=A_{1372}/A_{2900}$, where the absorption was estimated at 1372 cm^{-1} and 2900 cm^{-1}. As a baseline for the band at 2900 cm^{-1}, the height of the adjacent shoulder near 3000 cm^{-1} was chosen. For the band at 1372 cm^{-1}, a baseline was drawn between the maximum at approximately 1290 and 1410 cm^{-1} [10].

Thermograms were obtained using DTG 60H equipment (Shimadzu Scientific Instruments, Columbia, MD, USA) under an N_2 flux rate of 20 cc/min and at a heating ramp of 10°C/min from 30°C to 600°C. Differential thermal analysis (DTA) curves were collected by measuring the temperature difference between the sample pan and the reference pan. Differentiation thermogravimetric analysis (DrTGA) curves were calculated through obtaining the first derivative of the mass loss (TGA) by the equipment's TA60WS software.

RESULTS AND DISCUSSION

Figure 1 shows the surfaces of a cellulose membrane obtained from coelectrospinning deposition onto a rotating wire drum and onto a stationary metal screen. The wire drum rotation direction superimposed a preferential vectorial direction over the deposited cellulose fibers, although a number of fibers were still randomly deposited. The ability to maintain predominantly unidirectional control on fiber orientation via a simple rotating drum was a remarkably facile way to govern the critical aspect of orientation. The deposited cellulose fibers had a cellulose nanocrystals core that are then bonded to one another, forming a film with drastically more contact points between fibers than in the case of using a stationary metal screen as a collector.

We then analyzed the features of this orientational effect using much higher resolution than shown in Fig. 1. **Figure 2**

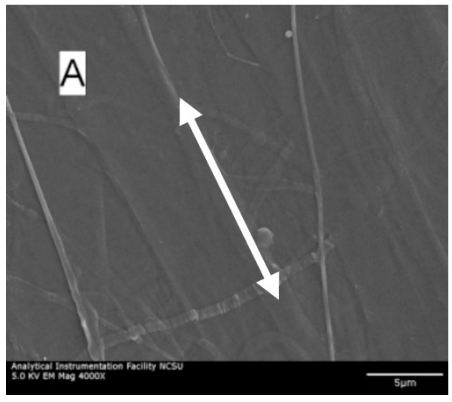

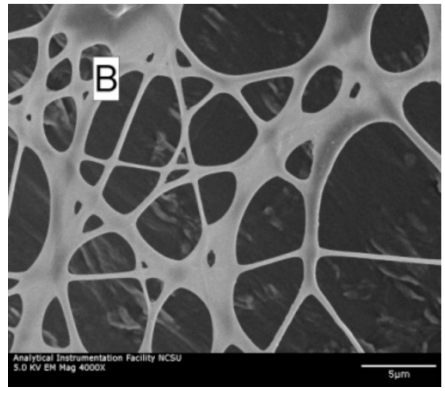

1. Field emission scanning electron microscopy (FE-SEM) of surface (A) film obtained at 10-cm distance from tip to rotating wire drum over water vapor; (B) mat obtained at 8-cm distance from tip to stationary metal screen at 4,000x magnification. The double arrow indicates the alignment direction.

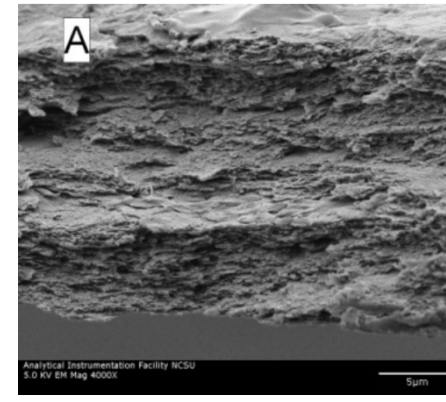

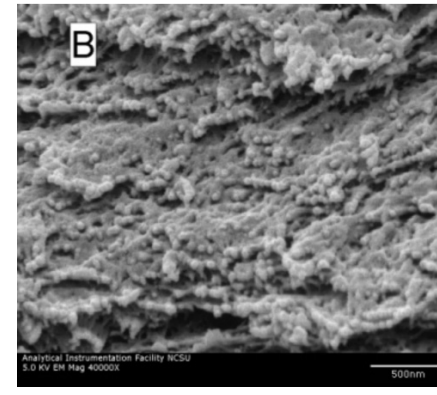

2. FE-SEM of mats obtained at 10-cm distance from tip to (A) rotate wire drum over water vapor, cross- section view at 4,000x magnification and (B) detail of A showing the lamellar structure at a cross-section of 40,000x.

illustrates a cross-section of similar nanofiber film obtained from collecting fibers onto a rotating wire drum. The film was fractured manually and subsequently analyzed by FE-SEM. The image shows that the fibers laid down on the film surprisingly achieved a quasi-lamellar configuration. When using a cellulose nanocrystals water suspension with a stationary metal screen collector, the cellulose nanocomposites agglomerated and were not well dispersed on the cellulose mats. Therefore, application of a simple rotating wire drum induced a vectorial directionality and uniformity of distribution for the cellulose nanocomposites within cellulose electrospun fibers.

Obtaining support for the material identities in the nanofibers was integral to validating our conclusions. **Figure 3** shows FTIR spectra of the films and mat obtained by coelectrospinning at three different conditions. The spectra present a typical signature for cellulose. The peak at 1111 cm^{-1} is quite strong and indicative of cellulose crystallinity type I, appearing only as a shoulder in cellulose II and amorphous cellulose due to the development of a strong, broad band near 1090 cm^{-1} [10, 11]. This peak can be observed in the spectra of samples made of cellulose reinforced with cellulose nanocrystals. The

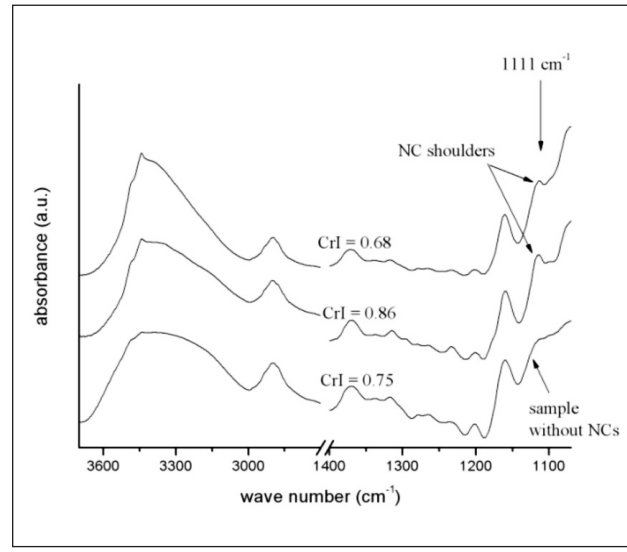

3. Fourier transform infrared (FTIR) spectra of the cellulose samples obtained by coelectrospinning; CrI is the crystalline index calculated from FTIR spectra (A_{1372}/A_{2900}).

	Wt% Cellulose Nanocrystal DMSO Suspension	Syringe Size Ratio (mL/mL)	Sheath/Core Flow Rate Ratio (cch^{-1}/cch^{-1})	Sheath Flow Rate (cc/h)	Total Flow Rate (cc/h)	Voltage (kV)	Distance to Rotate Wire Drum (cm)	Crystallinity Indices by FTIR A_{1372}/A_{2900}
Experiments with 2 wt% $NMMO.H_2O$ as solvent	1.56	10/1	9.4	1.98	2.19	16	10	0.67
	-	-	-	1.98	1.98	12	10	0.75
	-	-	-	1.19	1.19	12	10	0.73
Experiments with 3 wt% $NMMO.H_2O$ as solvent	1.56	10/1	9.4	1.98	2.19	25	10	0.86
	1.56	10/1	9.4	1.98	2.19	16	8	0.68
	1.56	10/1	9.4	1.98	2.19	16	10	0.52
	1.56	10/1	9.4	0.79	0.88	16	8	0.57
	-	-	-	1.19	1.19	16	10	-

I. Crystallinity of cellulose- and nanocrystals cellulose-reinforced cellulose fibers using FTIR absorption relationships.

FTIR spectra can be used to calculate the crystallinity index, which is generally in good agreement with X-ray diffraction (XRD) measurements [12, 13]. The absorption ratio with the best fit to XRD corresponds to the FTIR bands at 1372 and 2900 cm^{-1} and can be used to predict crystallinity even for a mixture of celluloses type I and II. **Table I** shows the relative crystallinity indices calculated from the FTIR spectra.

Increasing the amount of cellulose nanocrystals for reinforcement causes an increase in the FTIR crystallinity indices, as would be expected, because these indices correlate well with the crystallinity of a mixture of cellulose types I and II [13]. Yet, as shown in our previous work [8], samples with higher FTIR crystallinity indices were those without cellulose nanocrystals. In general, we have found that FTIR crystallinity indices increase with flow rate, ratio of shell to core, and applied voltage. Also, the flow rate of the shell does not affect the FTIR crystallinity indices for coelectrospinning experiments, despite the effect it has on spinnability. Past work indicates that cellulose type I does not induce increases in cellulose type II crystallization [14].

It has already been discussed that cellulose self-reinforced with partial dissolution and regeneration of cellulose type II showed increased tensile elastic modulus with crystallinity indices; however, the tensile strength was impaired at the highest crystallinity index [5]. Moreover, the degree of preferred orientation of cellulose nanocomposites increased both the tensile modulus and strength [6, 15].

The DTA and DrTGA of oven-dried cellulose nanocrystals are distinctly different from the thermograms of freeze-dried cellulose nanocrystals (**Fig. 4**). The main events that can be seen on the DrTGA curve were localized at approximately 194°C, 280°C, 460°C, and 502°C for the porous freeze-dried cellulose nanocrystals. The more compact cellulose nanocrystals films obtained by oven drying began thermal events approximately at 195°C with shoulders beyond 213°C (almost completely overlapped peaks) and 550°C. The DTA curve for oven-dried cellulose nanocrystals was composed of more overlapped signals than for the freeze-dried cellulose nanocrystals. In addition, a heat evolution was finished at 540°C for freeze-dried samples, unlike that for oven-dried cellulose nanocrystals samples. Films with a higher content of cellulose nanocrystals clearly displayed thermal events around 205°C and beyond 517°C as confirmed by both DTA and DrTGA curves. These peaks do not appear for the film made without cellulose nanocrystals. Moreover, the film with low cellulose nanocrystals content presented thermal event around 475°C with a shoulder at 502°C.

The majority of past studies simply considered the kinetics of cellulose thermal degradation into low temperature ranges (below 450°C) [16, 17]. At this temperature range, crystallinity [18], agglomeration of fibrils [19], allomorphism [18], and heating rate [20] affect thermal properties. Although Szczesniak and Rachocki [17] studied microcrystalline cellulose (66% crystallinity) powder oxidation in ambient conditions below 400°C, their DTA traces showed thermal events up until 475°C. Thermal degradation of cellulose nanocrystals under nitrogen should occur at higher temperatures than for other cellulose alomorphs because they are highly crystaline (>90%) with lattice type I.

Oven drying appeared to promote cellulose nanocrystal aggregates by increasing drastically the number of contact points (physical, chemical, or both) between cellulose nanocrystals. During pyrolysis, for example, it was found that dehydration occured with the formation of crosslinks [19, 20] that induced the degradation of the surrounding cellulose nanocrystals. Thus, thermal degradation of oven-dried cellulose nanocrystals was promoted and degradation was expected compared with the freeze-dried cellulose nanocrystals.

Thermal events beyond 500°C were attributed to char degradation whose yield depended on the aggregation state, alo-

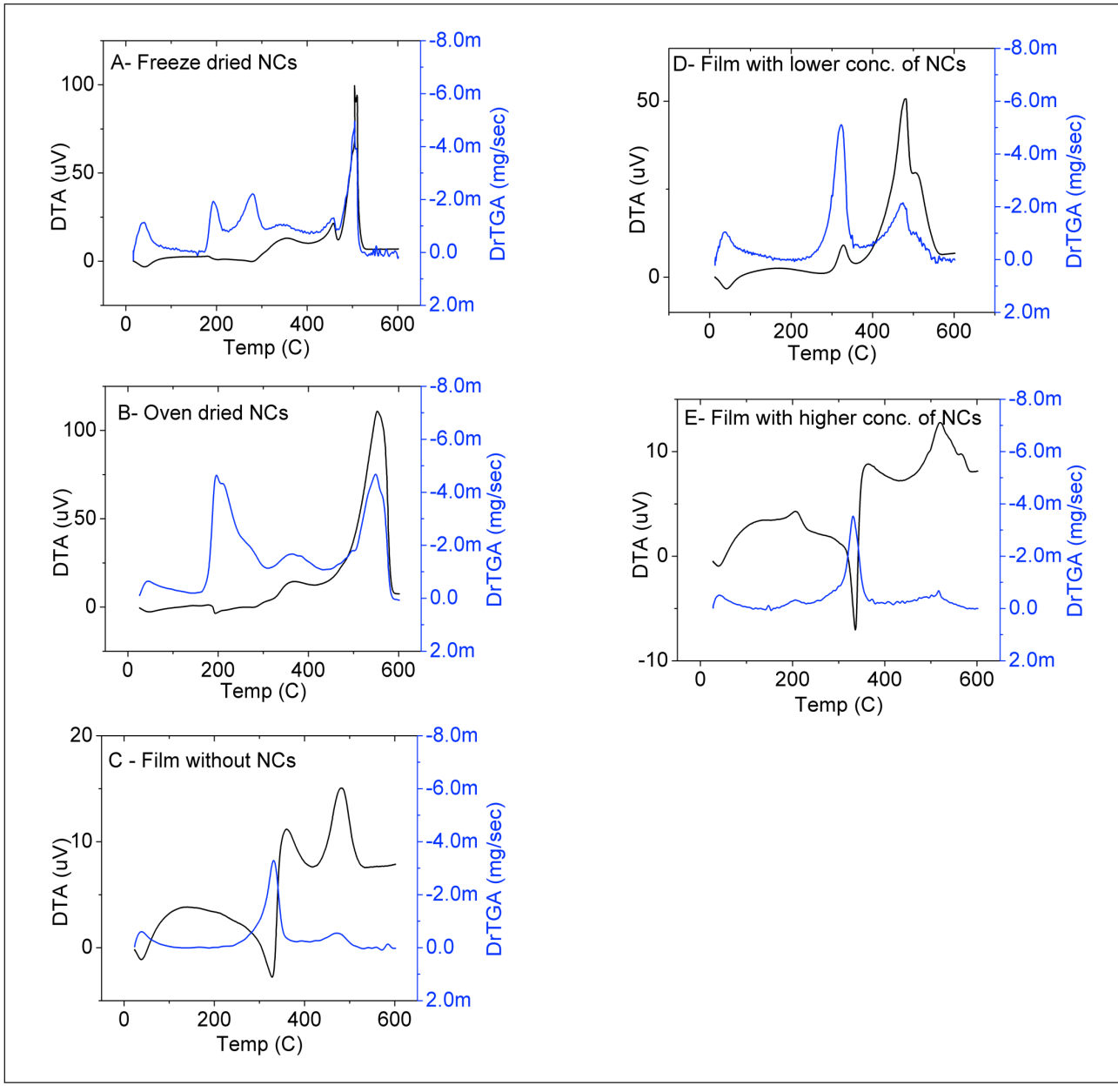

4. Differential thermal analysis (DTA) and differentiation thermogravimetric analysis (DrTGA) of (A) cellulose nanocrystals freeze dried from 3.28 wt% water suspension; (B) nanocrystals oven dried from 3.28 wt%; (C) mat without core from 2.00 wt% dope solution in NMMO.H_2O; (D) mat from flow rate ratio 9.4, 3.00 wt% dope solution in NMMO.H_2O, 1.56 wt% nanocrystals in DMSO suspension; (E) mat from flow rate ratio 9.4, 2.00 wt% dope solution in NMMO.H_2O, 1.56 wt% cellulose nanocrystals in DMSO suspension.

morphism, and crystallinity of the cellulose sample. Furthermore, when thermal degradation began at a lower temperature, char formation also occurred earlier.

Despite cellulose of crystallinity type I being much more easily observed in the FTIR spectra, in general, one characterization technique corroborated another. The DTA peak at 552°C (Fig. 4) for a fiber film with higher cellulose nanocrystals content was closer to a more loosely knit nanocrystal structure, as in the freeze-dried sample (**Fig. 5**). Conversely, when a cellulose nanocrystals water suspension was used for the core fluid, the cellulose nanorods agglomerated with no apparent mechanical reinforcement of the resultant mats [8].

Figure 5 shows the tensile mechanical stress-strain curves for electrospun (using the rotating wire drum) cellulose without and with nanocrystal reinforcement. The films were stretched 10% after NMMO and DMSO extraction with water. The cellulose films with reinforcement showed significant increases both in tensile MOE and in the tensile stress at maximum load. It is interesting to note that although the inclusion of cellulose nanocomposites substantially increased the mechanical properties, the crystallinity indices calculated by FTIR absorptions did not correlate. The unaligned cellulose

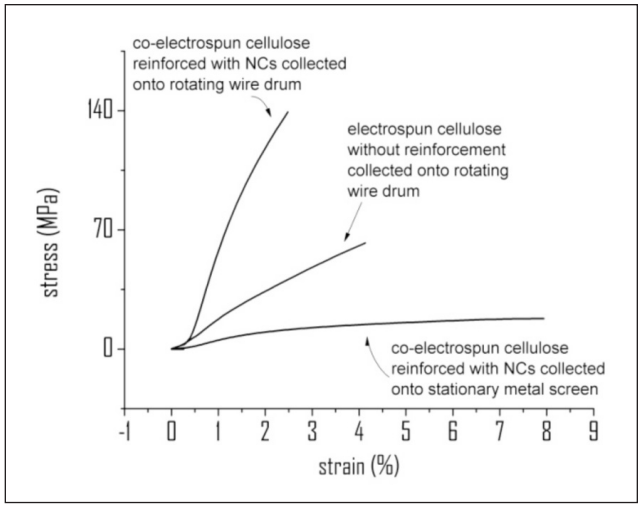

5. Tensile stress versus strain for films of coelectrospun cellulose with cellulose nanocrystals in the core and without reinforcement. Both were collected onto a rotating wire drum, whereas coelectrospun cellulose with reinforcement was collected onto a stationary metal screen.

mat collected onto the stationary metal screen presented high elongation at break and low tensile stress at maximum load.

Thus, an important fundamental finding of this study is that the orientation of the cellulose fibers, availability of well-dispersed cellulose nanocomposites, and the adhesion between fibers of cellulose type II is much more important for gains in tensile mechanical strength than relying exclusively on cellulose crystallinity.

CONCLUSIONS

A coelectrospinning apparatus was used to generate cellulose films reinforced by cellulose nanocrystals collected onto rotating wire drum. We found that well-dispersed cellulose nanocrystals inside nano- and microcellulose yarns could be obtained by using a DMSO suspension instead of a water suspension for the core cellulose nanocrystals suspension in coelectrospinning experiments. The current technique promotes alignment and adhesion of the amorphous cellulose fibers, thus playing a more important role in the mechanical properties of cellulosic films than the crystallinity index alone. **TJ**

ACKNOWLEDGEMENTS

We would like to acknowledge the Brazilian agency CNPq for the provision of a research fellowship to WLEM. We would also like to acknowledge Professors O. Rojas (forest biomaterials), E. Loboa (biomedical engineering), and the North Carolina State Metal Workshops for their assistance in developing

ABOUT THE AUTHORS

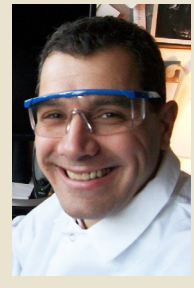

Lucia

Magalhães

Ramires

Cao

Cellulose composites have been a subject of intense interest in our laboratory for several years. The ability to demonstrate unique aspects of their physical properties within an electrospinning context was too attractive to pass up. Our work drew from the research of a number of noteworthy scientists in the areas of nanocellulose (e.g., Gray, Marchessault, Chanzy, Atalla, Heux, Dufresne) and electrospinning (e.g., Frey, Rojas). We then put our spin on it by combining the crystals and whole cellulose within a core-in-shell blend and cast aligning them on a rotating drum.

The most difficult aspect of our work was the physical construction of the core-in-shell apparatus and the rotating drum. This equipment was built in-house from readily available materials, and although it wasn't pretty, the system worked well!

We did get some remarkable results that we did not expect. We learned that it was possible to make core-in-shell all-cellulose composites whose cellulose shell displayed a higher crystallinity than the nanocrystals! For mills, the large-scale production of nanocrystals continues to be a challenge but there are numerous opportunities for composites. Although the work here is too fundamental for any realistic industrial application, it nonetheless offers a unique perspective on developing all-cellulose blends whose mechanical properties are tunable. We will continue to explore how other core materials influence the shell crystallinity.

Lucia is associate professor, Department of Forest Biomaterials, Laboratory of Soft Materials and Green Chemistry, North Carolina State University (NCSU), Raleigh, NC, USA. Magalhães is researcher with Embrapa Forestry, Colombo, PR, Brazil. Ramires is a graduate student in NCSU's Department of Forest Biomaterials in Raleigh. Cao is associate professor, Biomedical Engineering, South China University of Technology, Guangzhou, China. Email Lucia at lucian.lucia@ncsu.edu.

the equipment described. Finally, portions of this work would not have been possible without the generous support of a Higher Education Challenge Grant administered by the United States Department of Agriculture (Cooperative Agreement No. 2006-38411-17035.)

LITERATURE CITED

1. Nishino, T., Takano, K., and Nakamae, K., *J. Polym. Sci. Part B: Polym. Phys.* 33: 1647(1995).
2. Ishikawa, A., Okano, T., and Sugiyama, *J., Polymer* 38: 463(1997).
3. Lahiji, R.R., Xu, X., Reifenberger, R., et al., *Langmuir* 26(6): 4480(2010).
4. Nishino, T., Matsuda, I., and Hirao, K., *Macromolecules* 37: 7683(2004).
5. Gindl, W. and Keckes, *J., Polymer* 46: 10221(2005).
6. Gindl, W. and Keckes, J., *J. Appl. Polym. Sci.* 103 : 2703(2007).
7. Qi, H., Cai, J., Zhang, L., and Kuga, S., *Biomacromolecule* 10(6): 1597(2009).
8. Magalhães, W.L.E., Lucian, L.A., and Cao, X., *Langmuir* 25: 13250(2009).
9. Reznik, S.N., Yarin, A.L., Zussman, E., et al., *Phys. Fluids* 18: 062101-1(2006).
10. Nelson, M.L. and, O'Connor, R.T., *J. Appl. Polym. Sci.* 8: 1311(1964).
11. Carrillo, F., Colom, X., Sunol, J.J., et al., *Eur. Polym. J.*, 40: 2229(2004).
12. El-Wakil, N.A. and Hassan, M.L., *J. Appl. Polym. Sci.* 109: 2862(2008).
13. Nelson, M.L. and O'Connor, R.T., *J. Appl. Polym. Sci.* 8: 1325(1964).
14. Iyer, P.B., Sreenivasan, S., Chidambareswaran, P.K., et al., *Text. Res. J.* 54: 732(1984).
15. Gindl, W., Martinschitz, K.J., Boesecke, P., et al., *Compos. Sci. Technol.* 66: 2639(2006).
16. Mamleev, V., Bourbigot, S., and Yvon, J., *J. Anal. Appl. Pyrolysis* 80: 151(2007).
17. Szczesniak, L., Rachocki, A., and Tritt-Goc, *J., Cellulose* 15: 445(2008).
18. Ciolacu, D. and Popa, V.I., *Cellulose Chem. Technol.* 40(6): 445(2006).
19. Quievy, N., Jacquet, N., Sclavons, M., et al., *Polym. Degrad. Stab.* 95: 306(2010).
20. Chaiwat, W., Hasegawa, I., Tani, T., et al., *Energy Fuels* 23: 5765(2009).